

Portland State University

PDXScholar

Physics Faculty Publications and Presentations

Physics

2016

Atmospheric Methane Isotopic Record Favors Fossil Sources Flat in 1980s and 1990s with recent increase

Andrew L. Rice

Portland State University

Christopher Butenhoff

Portland State University, cbuten@pdx.edu

Doaa Galal Mohammed Teama

Portland State University

Florian H. Röger

Portland State University

M. A. K. Khalil

Portland State University, aslamk@pdx.edu

Follow this and additional works at: https://pdxscholar.library.pdx.edu/phy_fac



See next page for additional authors
Part of the [Physics Commons](#)

Let us know how access to this document benefits you.

Citation Details

Rice, A. L., Butenhoff, C. L., Teama, D. G., Röger, F. H., Khalil, M. A. K., & Rasmussen, R. A. (2016). Atmospheric methane isotopic record favors fossil sources flat in 1980s and 1990s with recent increase. *Proceedings of the National Academy of Sciences*, 113(39), 10791-10796.

This Conference Proceeding is brought to you for free and open access. It has been accepted for inclusion in Physics Faculty Publications and Presentations by an authorized administrator of PDXScholar. Please contact us if we can make this document more accessible: pdxscholar@pdx.edu.

Authors

Andrew L. Rice, Christopher Butenhoff, Doaa Galal Mohammed Teama, Florian H. Roger, M. A. K. Khalil, and R. A. Rasmussen

Atmospheric methane isotopic record favors fossil sources flat in 1980s and 1990s with recent increase

Andrew L. Rice^{a,1,2}, Christopher L. Butenhoff^{a,1}, Doaa G. Teama^a, Florian H. Röger^a, M. Aslam K. Khalil^a, and Reinhold A. Rasmussen^b

^aDepartment of Physics, Portland State University, Portland, OR 97207; and ^bDivision of Environmental and Biomolecular Systems, Oregon Health & Science University, Portland, OR 97239

Edited by Mark H. Thiemens, University of California, San Diego, La Jolla, CA, and approved July 26, 2016 (received for review November 19, 2015)

Observations of atmospheric methane (CH₄) since the late 1970s and measurements of CH₄ trapped in ice and snow reveal a meteoric rise in concentration during much of the twentieth century. Since 1750, levels of atmospheric CH₄ have more than doubled to current globally averaged concentration near 1,800 ppb. During the late 1980s and 1990s, the CH₄ growth rate slowed substantially and was near or at zero between 1999 and 2006. There is no scientific consensus on the drivers of this slowdown. Here, we report measurements of the stable isotopic composition of atmospheric CH₄ (¹³C/¹²C and D/H) from a rare air archive dating from 1977 to 1998. Together with more modern records of isotopic atmospheric CH₄, we performed a time-dependent retrieval of methane fluxes spanning 25 y (1984–2009) using a 3D chemical transport model. This inversion results in a 24 [18, 27] Tg y⁻¹ CH₄ increase in fugitive fossil fuel emissions since 1984 with most of this growth occurring after year 2000. This result is consistent with some bottom-up emissions inventories but not with recent estimates based on atmospheric ethane. In fact, when forced with decreasing emissions from fossil fuel sources our inversion estimates unreasonably high emissions in other sources. Further, the inversion estimates a decrease in biomass-burning emissions that could explain falling ethane abundance. A range of sensitivity tests suggests that these results are robust.

atmospheric methane | greenhouse gas emissions | methane isotopic composition | methane trends | Bayesian inversion

Considerable research since the 1970s has established the role of methane (CH₄) in climate, as an infrared active gas, and as a chemically reactive species affecting hydroxyl radical, ozone, and carbon monoxide in the troposphere and chlorine, ozone, and water vapor in the stratosphere. At a globally averaged mixing ratio of 1,800 ppb, the abundance of CH₄ in the atmosphere has more than doubled since the industrial revolution as a result of population growth, agricultural practices, and fossil fuel use (1). The rise in CH₄ concentration is considered to contribute 0.48 Wm⁻² of the 2.83 Wm⁻² radiative forcing by well-mixed greenhouse gases since 1750 (2). Including indirect effects from CH₄ emissions roughly doubles its effective radiative forcing. Its global warming potential (not including feedbacks) is 28 based on a 100-y time horizon, but 84 based on a 20-y timescale [global warming potential (GWP) is relative to CO₂], illustrating the potential of large changes in the burden of CH₄ to influence climate on short timescales (2).

Both the decrease in the CH₄ growth rate and its interannual variability since 1984 are well documented by at least four global networks of atmospheric measurements; agreement between time series is excellent with some exceptions early on. Recently, a review and synthesis of the CH₄ budget (3) pointed to some consensus of measurement and modeling studies and their comparisons toward understanding temporal changes in the CH₄ budget. In agreement with previous work, this study showed that decadal-scale CH₄ concentrations are consistent with nearly no secular trend in global CH₄ emissions over the past three decades until the recent uptick (4, 5). Modeling studies, in general,

show that interannual variability is driven primarily by natural wetland emissions, both tropical and boreal, the largest of the natural CH₄ sources.

However, disagreement remains over the magnitudes and, importantly, the trends in CH₄ source categories during this period of atmospheric growth rate decline. In particular, two recent studies using the tracer ethane have linked a sustained drop in ethane mixing ratios to a decrease in fugitive fossil fuel-based CH₄ emissions by 10–30 Tg y⁻¹ since the 1980s (6, 7). This top-down result differs with bottom-up emissions inventories that show increasing or flat fugitive fossil fuel CH₄ emissions (8). Contemporaneously, other work (9) used trends in the interhemispheric gradient in the carbon isotopic composition (δ¹³C) of CH₄ to infer that biogenic CH₄ sources of CH₄ declined over the period 1984–2005, which authors link to ~16 Tg y⁻¹ decrease in rice agricultural emissions. This agrees with several bottom-up studies (10, 11). However, this claim was challenged by an analysis of new and existing δ¹³C of CH₄ results that do not show such a trend (12). A synthesis of available information seems to favor “decreasing-to-stable” fugitive fossil fuel CH₄ sources during the 1980s and 1990s (3), a conclusion that is supported by a very recent box-model analysis (13). What is noteworthy, however, is that in either case of fossil or rice sources, a long-term decrease in one source category would require an increase in another to balance the total global CH₄ budget over the period.

Significance

There is no scientific consensus on the drivers of the atmospheric methane growth rate over the past three decades. Here, we report carbon and hydrogen isotopic measurements of atmospheric methane in archived air samples collected 1977–1998, and modeling of these with more contemporary data to infer changes in methane sources over the period 1984–2009. We present strong evidence that methane emissions from fossil fuel sectors were approximately constant in the 1980s and 1990s but increased significantly between 2000 and 2009. This finding challenges recent conclusions based on atmospheric ethane that fugitive fossil fuel emissions fell during much of this period. Emissions from other anthropogenic sources also increased, but were partially offset by reductions in wetland and fire emissions.

Author contributions: A.L.R., C.L.B., and D.G.T. designed research; A.L.R., C.L.B., D.G.T., F.H.R., and M.A.K.K. performed research; D.G.T., F.H.R., and R.A.R. contributed new reagents/analytic tools; A.L.R., D.G.T., F.H.R., and M.A.K.K. analyzed data; and A.L.R. and C.L.B. wrote the paper.

The authors declare no conflict of interest.

This article is a PNAS Direct Submission.

Data Deposition: Air archival methane isotope data are available at the Carbon Dioxide Information Analysis Center and the World Data Centre for Greenhouse Gases, or can be obtained by contacting the corresponding author (A.L.R.).

¹A.L.R. and C.L.B. contributed equally to this work.

²To whom correspondence should be addressed. Email: arice@pdx.edu.

This article contains supporting information online at www.pnas.org/lookup/suppl/doi:10.1073/pnas.1522923113/-DCSupplemental.

Isotopic information is particularly useful as a direct means to constrain and to interpret temporal changes in the CH₄ budget due to characteristic isotope ratios in major CH₄ sources: wetlands, rice and ruminant emissions $\delta^{13}\text{C} \sim -60\text{‰}$ $\delta\text{D} \sim -300\text{‰}$; fugitive fossil fuel emissions $\delta^{13}\text{C} \sim -40\text{‰}$ $\delta\text{D} \sim -175\text{‰}$; biomass-burning emissions $\delta^{13}\text{C} \sim -20\text{‰}$ $\delta\text{D} \sim -200\text{‰}$ (*SI Appendix, Table S1*). Despite the promise of isotopic CH₄ to help constrain the CH₄ budget, the scientific community is historically data limited; before ~ 1998 there were few isotopic CH₄ time series available and none that spanned decadal lengths (12, 14–17). This is particularly true for δD , for which very little data are available at all before the turn of the century.

To fill this void, we analyzed a rare archive of more than 200 air samples collected at Cape Mearns, Oregon (CM; 45.5°N, 124.0°W) between 1977 and 1998 to examine trends in the dual-tracer isotopic composition ($\delta^{13}\text{C}$ and δD) of atmospheric CH₄. An additional 100 archive samples measured were from sites including: Mauna Loa (21.1°N, 157.2°W) and Cape Kumukahi (19.3°N, 154.5°W), Hawaii (1992–1996); Tutuila, American Samoa (14.1°S, 170.6°W, 1995); South Pole (90°S, 1992–1995); and Sable Island, Nova Scotia (43.9°N, 60.02°W, 1992).

To infer changes in the CH₄ budget for the years 1984–2009 we used the chemical transport model GEOS-Chem (18) at 4° × 5° spatial resolution and performed a Bayesian inversion of atmospheric observations of CH₄ mixing ratio using monthly CH₄ mixing ratios at 221 sites from the National Oceanic and Atmospheric Administration (NOAA) Earth System Research Laboratory GLOBALVIEW-CH₄ data product (19) and $\delta^{13}\text{C}$ from several observational networks including the current work, the Institute of Arctic and Alpine Research (20), Quay et al. (16), and Tyler et al. (17).

Results

Three-Decade Record of Isotopic CH₄. The resulting isotopic measurements at CM constitute one of the longest continuous records of the isotopic composition of methane and date back to a time when no other time series data are available (late 1970s

and early 1980s). This is an important time for understanding the CH₄ budget, as the CH₄ growth rate is in a sustained multidecadal decline. To create a more than three-decade uninterrupted record of isotopic CH₄, which extends to near-present time, we combine historic $\delta^{13}\text{C}$ data from CM with published datasets from mid-latitude North America from Olympic Peninsula, Washington (CPO; 48°N, 126°W, 1988–1996; ref. 16), Montaña de Oro, California (MDO; 35°N, 121°W, 1996–2006; ref. 17) and Niwot Ridge, Colorado (NWR; 40°N, 105°W, 1994–2010; refs. 15, 17). The δD time series from CM were combined with existing data from MDO and NWR (2000–2006; ref. 17). These locations were found to have comparable behavior in their seasonal cycles and long-term trends over periods of overlap. Because absolute values in concentration, $\delta^{13}\text{C}$ and δD vary spatially, mean values were adjusted using periods of overlap between datasets (*SI Appendix, section S.2*). This approach also accounts for small adjustments resulting from calibration differences between laboratories, found to be critical in previous work (12). Together with the long-standing CH₄ concentration record, this composite record from the midlatitude Northern Hemisphere provides a record of the secular and seasonal trends in isotopic CH₄ as well as some of the interannual variability (Fig. 1).

This composite Northern Hemisphere record captures the slowdown of the CH₄ growth rate, well-characterized over the past three decades (Fig. 1 *A* and *D*). Decadally averaged growth rates were found to be within the range of NOAA, Advanced Global Atmospheric Gases Experiment (AGAGE), University of California, Irvine (UCI), and Commonwealth Scientific and Industrial Research Organization (CSIRO) historical records (3), 15.1 ± 4.0 ($\pm 95\%$ CI) ppb y⁻¹ during the 1980s, 6.1 ± 2.3 ppb y⁻¹ during the 1990s, and 3.5 ± 1.1 ppb y⁻¹ during the 2000s (2.7 ± 1.0 ppb y⁻¹, 2000–2006; 4.6 ± 1.3 ppb y⁻¹, 2006–2010). The agreement between this composite midlatitude Northern Hemisphere dataset and the global mean derived from global monitoring datasets is due to the long lifetime of CH₄ in the atmosphere (~ 9 y) and resulting low spatial variability. Interannual variability in the CH₄ growth rate is also captured in most years, compatible with the NOAA global network (21) (Fig. 1*D*; $r^2 = 0.64$).

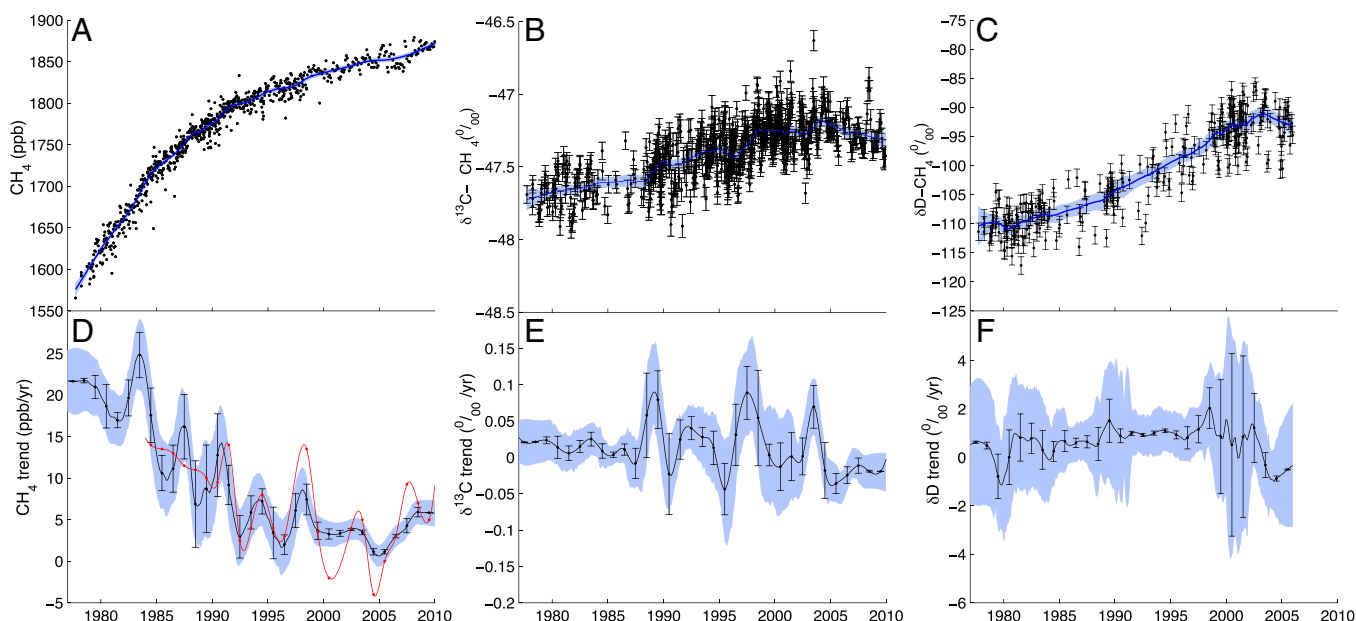


Fig. 1. Northern Hemisphere middle latitude composite dataset of CH₄ mixing ratio (*A*), $\delta^{13}\text{C}$ (*B*), δD (*C*), and their trends (*D–F*) 1977–2010. Raw data from CM, CPO, MDO, and NWR were deseasonalized and merged using periods of overlap to adjust each site relative to CM by a scalar. Fits (blue lines) were generated using a locally weighted regression technique (Lowess) and residual variability was bootstrapped to calculate uncertainty in the resulting trends (shaded region shown as 95% CI). Data points in trends (*D–F*) are annual mean values and error bars indicate 95% confidence intervals. CH₄ growth rate from the NOAA Earth System Research Laboratory - Global Monitoring Division (ESRL-GMD) (21) global network is shown in red (*D*) over the period 1984–2010 for comparison purposes.

The consistency between CH₄ time series from these composite CH₄ data and global networks provides confidence that observed temporal trends in the time series from the composite CH₄ isotope dataset reflect global trends rather than regional ones. Both δ¹³C and δD isotopic datasets show distinct behavior from CH₄ mixing ratio (Fig. 1 B and C). Beginning near −47.7‰ and −110‰ in the late 1970s, δ¹³C and δD increase with mean trends of 0.021 ± 0.019‰ y^{−1} and 0.59 ± 0.28‰ y^{−1} respectively (±95% CI) in the 1980s and 0.022 ± 0.027‰ y^{−1} and 1.02 ± 0.24‰ y^{−1} in the 1990s (Fig. 1 E and F). Maximum values of δ¹³C and δD of −47.2‰ and −95‰ are reached in the early 2000s followed by a leveling off or slight decrease in both isotopic tracers during the 2000–2005 period, which experienced a general stabilization of CH₄ mixing ratios. The rate of change in δ¹³C and δD after the year 2000 averaged −0.01 ± 0.029‰ y^{−1} (2000–2010) and −0.2 ± 1.4‰ y^{−1} (2000–2006), respectively.

Model Inversions. The match between optimized-model (a posteriori) and observations of CH₄ concentration and δ¹³C for all fixed sites is shown in *SI Appendix, Fig. S2*. The paucity of historical δD measurements limited its utility as a source constraint and δD was withheld from model inversions in favor of an additional a posteriori model validation (*SI Appendix, Fig. S3*). The effects of a wide array of more than 50 sensitivity tests (*SI Appendix, Table S4*) provides an assessment of uncertainty of inferred mean annual source fluxes (*SI Appendix, Table S1*) and

in temporal trends of sources (*SI Appendix, Fig. S4*). Sensitivity scenarios did change mean annual flux strengths in the CH₄ budget as perturbations to the base scenario require source flux adjustments to rebalance both the total and isotopic budgets (*SI Appendix, Table S1*). This is most evident when we perturbed both the isotopic fractionation of atmospheric CH₄ and the total CH₄ budget by altering sink processes. For example the addition of an isotopically fractionating marine boundary layer chlorine sink (*SI Appendix, scenario S6.1*) reduced emissions from the isotopically enriched biomass-burning source (−20 Tg y^{−1}) and increased emissions from the isotopically depleted biogenic source (+40 Tg y^{−1}). The opposite effect was true when we decreased the kinetic isotope effect of the OH sink (*SI Appendix, scenario S7*, see *SI Appendix section S.6* for details). However, the effect of most sensitivity scenarios on decadal-scale trends inferred from the data is minimal and the results of the base case appear robust (Fig. 2, *SI Appendix, Fig. S4*). Further, trends inferred in broader source categories with similar isotopic composition (e.g., all biogenic emissions) show smaller ranges than for individual source categories (*SI Appendix, Fig. S4*).

Results of the inversion analysis indicate the emission rate of anthropogenic sources (not including biomass burning) increased by 40 [16, 62] Tg y^{−1} (range given for 10th and 90th percentiles of sensitivity analyses) over the 25-y study period, with significant increases in fugitive fossil fuel (24 [18, 27] Tg y^{−1}), ruminant livestock (9 [4, 14] Tg y^{−1}), and waste management emissions (19

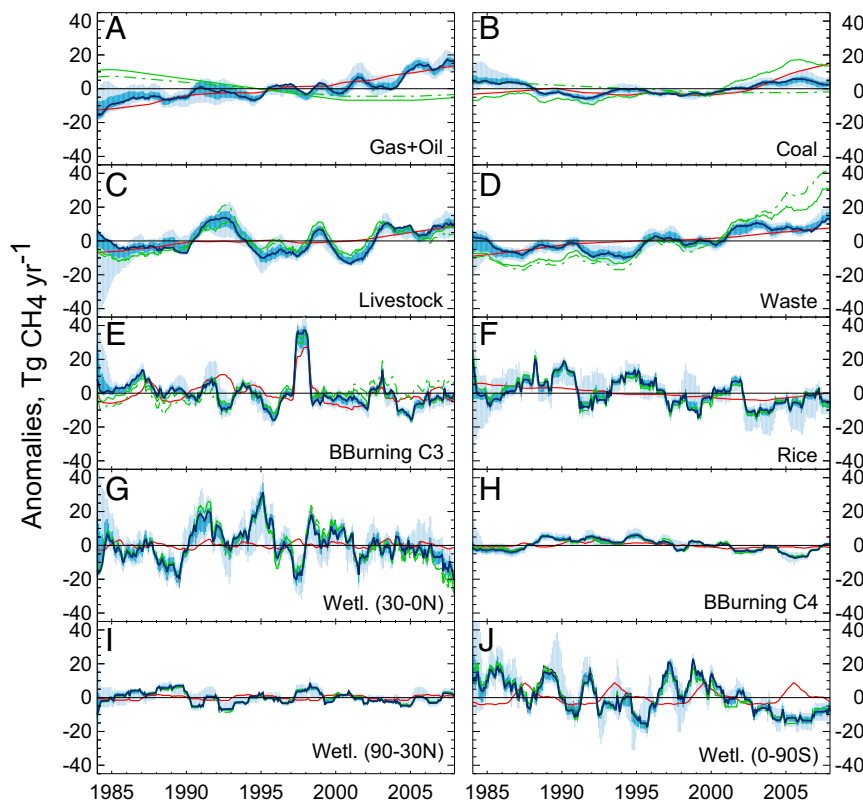


Fig. 2. Emissions anomalies for all 10 source categories. Anomalies were calculated by removing the long-term mean over the entire simulation period from the 12-mo running average of the emissions. Results from the base inversion are shown with the heavy dark blue line, and the red line indicates the prior emissions. The light blue shading shows the entire range of all 53 sensitivity runs in the ensemble and is therefore a representation of the “external” error of the inversion. Eighty percent of the ensemble is contained within the smaller darker blue shading indicating that biases from most sensitivity runs were small. The green lines are inversions where the fossil fuel emissions were fixed according to a scenario by Simpson et al. (7) based on measurements of atmospheric ethane (main text). The solid green line shows the inversion where all fossil fuel emissions were assigned to the gas + oil category and coal emissions and all other sources were optimized, and in the dashed green line inversion, both gas + oil and coal emissions were fixed based on a 65/35 split of the fossil fuel emissions. Individual plots show emissions anomalies from (A) gas and oil, (B) coal, (C) livestock, (D) waste, (E) biomass burning from C3 vegetation, (F) rice agriculture, (G) wetlands from 0 to 30°N, (H) biomass burning from C4 vegetation, (I) wetlands from 30°–90°N, and (J) wetlands from 0 to 90°S.

[15, 25] Tg y⁻¹). Wetlands were the largest contributor to interannual variations in CH₄ emissions and growth rate (Fig. 2). Within this variability, little change is inferred in the secular trend of the wetland source 1984–2000 (6 [–4, 11] Tg y⁻¹ increase). However, the following decade (2000–2009) experienced a significant decrease (29 [25, 32] Tg y⁻¹) in wetland CH₄ emissions continuing a trend inferred by Bousquet et al. (22). We find that rice emissions, although highly variable, do decrease significantly (12 [8, 17] Tg y⁻¹; Fig. 2*F*.) over the entire modeled period 1984–2009, consistent with bottom-up assessments (10, 11). The contribution of biomass-burning emissions toward interannual variability is minor except during the 1997–1998 anomaly in good agreement with previous top-down constraints but differing from bottom-up estimates, which tend to emphasize its role (3). However, excluding this large anomaly we find decreasing emissions from biomass burning of 14 [12, 18] Tg y⁻¹ over the period 1984–2009. Although there is no consensus from bottom-up fire inventories on the long-term trends in CH₄ emissions from biomass burning (23), we note evidence of decreasing burned area from fires in recent decades, supportive of this result (24, 25). Initially higher than the priors during the mid 1980s, combined fugitive fossil fuel CH₄ emissions (natural gas, oil, and coal) are flat during the period 1984–2000 consistent in trend with Emissions Database for Global Atmospheric Research (EDGAR) emissions inventories (4 [–5, 5] Tg y⁻¹). Subsequent to 2000, fugitive fossil fuel emissions increased by 21 [15, 24] Tg y⁻¹ over the next 9 y. Further, inversion results indicate growth in natural gas and oil sectors over the entire modeled period 1984–2009 (21 [16, 24] Tg y⁻¹ increase) contrasted by coal, which experienced a decrease in the 1980s followed by a leveling off in the 1990s (7 [5, 10] Tg y⁻¹ decrease, 1984–2000) and a small increase in the 2000s (5 [4, 7] Tg y⁻¹ increase, 2000–2009). Both recent increases in coal emissions, from increased mining in China, and increased natural gas emissions, from the onset of large-scale hydraulic fracturing of shale gas, are substantiated by recent studies and emissions inventories (8, 21, 26). Early in the 2000s, a coincident strong decrease in wetland emissions keeps total CH₄ emissions stable, but the end of this trend combined with growing emissions from livestock, waste, and fossil fuel industry lead to an uptick in the global CH₄ sources after 2005.

Optimized forward model results (using base scenario emissions derived from CH₄ and δ¹³C observations) for CM, MDO, and NWR for δD (Fig. 1*C*) provide a final assessment of model bias. Seasonality and secular trend are well matched with the composite northern hemispheric dataset for the majority of the observational period (*SI Appendix, Fig. S3*), illustrating that the model simulations represent withheld data well overall. However, there is some discrepancy in the last 2 y of the time series where observations of δD level off yet modeled δD continues to rise. This contrasts optimized modeled δ¹³C, which shows a leveling off during this period consistent with observations. The mismatch of modeled δD late in the time series may be in part due to the assigned δD isotopic signatures of sources (*SI Appendix, Table S1*), which are more poorly constrained than δ¹³C. Modeling sensitivity studies that decreased the isotopic signatures (δD) of CH₄ sources (wetlands, biomass-burning, and fossil fuel emissions) reproduced the δD trend late in the time series; however, these model runs resulted in a decrease in the match with observations overall by decreasing modeled δD isotopic composition over the entire period (*SI Appendix, Fig. S5*).

Discussion

Comparison of Model Inversion with Prior Studies. Consistent with earlier work and a recent synthesis that calculates the global CH₄ source at 551 Tg y⁻¹ 1980–1989, 554 Tg y⁻¹ 1990–1999, and 548 Tg y⁻¹ 2000–2009 (3), the composite northern hemispheric middle latitude methane concentration dataset (Fig. 1*A* and *D* showing an exponential decay in the CH₄ growth rate) and our global model inversion is broadly consistent with substantial interannual

variability but absence of any substantial secular trend in the total global CH₄ source over the past three decades (through 2006). It is telling, however, that the secular trends observed in isotopic CH₄ do not show a similar asymptotic behavior and fall below trends toward steady-state equilibrium indicating a shift among sources within a roughly constant global total. A simple time-dependent mass-balance approach based on observed δ¹³C and δD and their trends in time (Fig. 1) indicates that source isotopic composition was in decline over the period 1978–2009 (δ¹³C ~ 0.3‰, δD ~ 3‰; *SI Appendix, Fig. S6*). This result is supported by the full global model inversion, which also infers a falling global mean δ¹³C of emissions of the same rate (1984–2009; *SI Appendix, Fig. S6*). These isotopic trends are qualitatively consistent with some changes in the CH₄ budget over the three-decade period, specifically relative decreases in one or more isotopically enriched sources (i.e., fossil fuel or biomass burning) and relative increases in isotopically depleted sources (i.e., natural wetlands, agricultural or waste; *SI Appendix, Table S1*) keep global emissions roughly constant.

There is independent evidence in studies for declines in both CH₄ emissions from global biomass-burning (25) and fugitive fossil fuel emissions (27) over the past few decades. However, there is disagreement on this topic and other studies infer increasing trends in these sources (8, 28). Global-scale model inversion results presented here favor a decrease in fire CH₄ emissions due in part to leverage on the isotopic budget of CH₄ resulting from their enriched δ¹³C signature (*SI Appendix, Table S1*), i.e., a change in fire emissions will result in a larger shift in δ¹³C than an equivalent change in fugitive fossil fuel emissions. Predominantly located in the tropics, a global decrease in biomass-burning emissions also has little impact on the meridional distribution of CH₄.

Of isotopically depleted sources, natural wetlands are the largest source at ~165 Tg y⁻¹. Some bottom-up studies indicate upward decadal-scale trends in global wetland emissions (29), but top-down estimates using ground-based observations and satellite-based products combined with atmospheric models tend to favor constant or declining wetland emissions over the past few decades (3), consistent with this work. Global CH₄ emissions from solid waste are generally considered to have increased over the past few decades from increases in landfilled solid waste, even as CH₄ recovery increased (8, 30). Emissions from ruminant animals are also generally recognized to have risen over the past few decades due to increased populations of livestock (8, 31). Increases in both waste emissions and livestock emissions, which contribute to observed trends in δ¹³C and δD, are supported by inversion results here over the 1984–2009 period (19 [15, 25] and 9 [4, 15] Tg y⁻¹ respectively; Fig. 2*C* and *D*).

Finally, several bottom-up emissions inventories indicate a significant decrease in rice CH₄ emissions in recent decades (10, 11). This result is corroborated by inversion results here, which show a decrease in rice emissions (12 [8, 17] Tg y⁻¹ decrease over the period 1984–2009; Fig. 2*F*). Although rice emissions are isotopically depleted, and a decrease in rice emissions alone would increase the average global source δ¹³C, modeling results suggest that this change is offset by increasing emissions from waste and livestock categories and decreasing emissions from biomass burning. Notably, a decrease in rice emissions is inferred by our model without a significant change in the interhemispheric gradient in δ¹³C and δD (*SI Appendix, Fig. S7*), consistent with Levin et al. (12). An interhemispheric gradient observed in δ¹³C was proposed by Kai et al. (9) as evidence of a decrease in global rice emissions. Based on our analyses, either the decrease in rice emissions is masked by concomitant increases in waste and livestock categories or the interhemispheric gradient in δ¹³C is somewhat insensitive to changes in rice emissions, which are primarily at low latitudes (8).

Clearly some unresolved differences remain between approaches that assess changes in the CH₄ budget over the past few decades. It is particularly difficult to reconcile the results here with the assertion of decreasing (10–30 Tg y⁻¹) natural gas and

oil fugitive emissions based on falling ethane mixing ratios (6, 7). This scenario was selected as more likely than decreasing microbial emissions to explain the stabilization of CH₄ emissions in a recent review synthesis (3). To further investigate this hypothesis, we tested two scenarios based on falling ethane mixing ratios [storyline S₁ and S'₁ from Kirschke et al. (3)]. They first fixed gas and oil fugitive CH₄ emissions to the scheme derived from the ethane dataset requiring a decrease of 18 Tg y⁻¹ over the period 1985–2000, increasing 2 Tg y⁻¹ over the period 2000–2009 (a decrease of ~40 Tg y⁻¹ from our modeled base case over the entire period). This forcing of our model inversion resulted in an increase in coal fugitive emissions of ~20 Tg y⁻¹ over the base case (Fig. 2B, ~50% rise in coal emissions) and an increase from landfills and waste treatment of ~25 Tg y⁻¹ over the base case (Fig. 2D, >50% increase in source) for the entire period (1984–2009). Both fugitive emissions from coal mining and waste emissions (EDGAR 4.2) have a similar meridional distribution to fugitive natural gas emissions, and the combination of the two maintains the source δ¹³C isotopic composition. In this scenario, small additional changes are also inferred in rice emissions, biomass-burning emissions, livestock emissions, and wetland emissions that satisfy mass balance (Fig. 2). Large increases in coal and waste emissions are outliers in emissions inventories and on the high-end of sensitivity tests (Fig. 2B and D). The combination of decreasing natural gas and oil emissions in this scenario and increasing coal emissions results in nearly unchanged fugitive fossil fuel emissions over the period 1984–2009. With both fugitive CH₄ and ethane emissions occurring in coal mining, this scenario is unlikely to help explain the drop in ethane abundance over the period (6, 7).

Second, noting the incompatibility of increasing fugitive ethane (and CH₄) emissions in coal mining with the ethane record, we apportioned the 18 Tg y⁻¹ decrease in fugitive emissions between the two fossil fuel categories over the period 1985–2000 followed by a 2 Tg y⁻¹ rise (2000–2009); this scenario is still compatible with storylines S₁ and S'₁ from Kirschke et al. (3) (a decrease of ~40 Tg y⁻¹ compared with our base-case inversion). Under this scenario, the inversion response was to apportion an increase of ~35 Tg y⁻¹ into waste and landfill CH₄ emissions over the base case (Fig. 2D; ~100% increase in source), a ~20 Tg y⁻¹ increase in biomass burning over the base case (Fig. 2E and F; ~40% increase in source) and a decrease in wetland and rice emissions (~15 Tg y⁻¹) from the base case (Fig. 2). In this scenario, waste emissions maintain the source meridional distribution, and biomass-burning emissions balance the δ¹³C flux. Although mathematically possible within the ~500 Tg y⁻¹ CH₄ budget, there is little bottom-up support for the required rapid rise in waste and landfill CH₄ emissions (3).

Without falling fugitive fossil fuel emissions is it possible to explain falling atmospheric ethane abundance? Notably, our base-inversion result of declining biomass-burning emissions could satisfy CH₄, isotopic CH₄, and ethane trends over the period 1984–2009 (Fig. 3). Specifically, applying a calculated 14 Tg y⁻¹ decline in biomass-burning CH₄ emissions from our base inversion and a weighted mean CH₄ to ethane ratio in fire of 5:1 (32) results in a 3 Tg y⁻¹ decrease in ethane emissions compatible with the observed decrease in atmospheric ethane abundance (7). However, we note that emitted CH₄-to-ethane ratios are variable and better knowledge of global average CH₄-to-ethane ratios in fugitive emissions by gas, oil, and coal subsectors and in biomass-burning emissions would be particularly helpful in resolving this issue further.

Implications. Overall, we emphasize that although the CH₄ growth rate went through a dramatic decline over the past three decades, a decline in CH₄ sources is not needed to balance sources and sinks (5). Nonetheless, there is evidence that source apportionment shifted during this period, which fundamentally

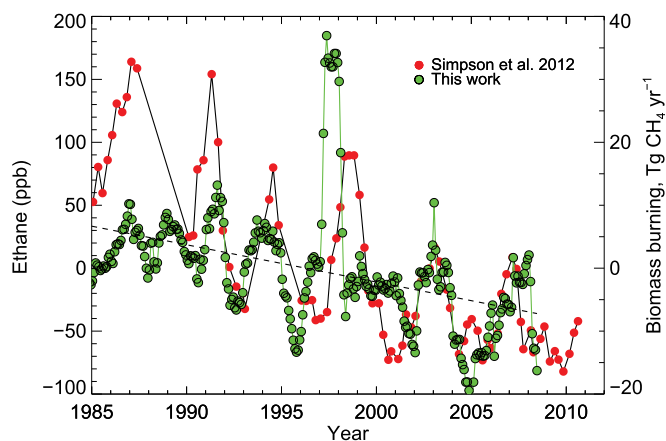


Fig. 3. Interannual anomaly in atmospheric ethane [red circles, from Simpson et al. (7)] and the posterior monthly deseasonalized biomass burning (C3 + C4) CH₄ emissions from the present study (green circles). The dashed line is a linear fit to the biomass-burning emissions with a slope of $-0.59 \text{ Tg CH}_4 \text{ yr}^{-1}$ ($\pm 0.15 \text{ Tg yr}^{-1}$, 95% CI).

requires that a secular change in one source category must be met by a change in equal magnitude and opposite sign in other sources. Global observations of CH₄ concentration, including its trends and spatial distribution, and trends in CH₄ isotopic composition (δ¹³C and δD) provide a top-down constraint to our understanding of how CH₄ sources have changed over the past three decades. Accordingly, 3D global chemical transport models fully use these components and are most useful in the endeavor to best match sources with observations.

The Bayesian inversion performed here using the Goddard Earth Observing System (GEOS)-Chem global chemical transport model demonstrates the utility of long-term isotopic measurement records together with long-standing measurements of CH₄ concentration toward constraining changes in the budget of CH₄. This capacity will increase with current and future isotopic observations. Our work here focuses on the period 1984–2009, and finds a significant increase in the anthropogenic source of CH₄ from 2000, despite being mainly flat in the 1980s and 1990s. CH₄ interannual variability is dominated by wetland emissions, which show very little long-term changes through 2000, but decrease after 2000, in agreement with previous work on the subject (22). Further, our measurement-modeling approach favors a scenario of declining rice emissions over the period 1984–2000, as proposed previously (9), but challenged based on the interhemispheric gradient in δ¹³C (12). We find a scenario of decreasing fugitive fossil fuel emissions from 1984 to 2000 unlikely within the observational constraint without a substantial increase in landfill and waste CH₄ emissions. Finally, our study finds a decline in global biomass-burning emissions (excluding 1997–1998) over the nearly three-decade period. This result can explain declining global ethane abundance over the period 1984–2000 with roughly constant fugitive fossil fuel emissions.

Methods

Air Archive. Samples analyzed in this work were aliquots of historic air samples obtained from the Oregon Health and Sciences University Division of Environmental and Biomolecular Systems (SI Appendix, section S.1).

Analyses. Archive air samples were analyzed for CH₄ concentration using gas chromatograph with a flame ionization detection (33) to investigate sample stability in storage (SI Appendix, section S.1, Fig. S1). Measurements of δ¹³C and δD of CH₄ were made by continuous-flow gas chromatography isotope ratio mass-spectrometry on a Thermo Scientific Delta V IRMS as described previously (34, 35) (SI Appendix, section S.1). [Note, by convention, isotope ratios are expressed using the delta notation (as δ values), where

$\delta = [(R_{\text{sample}}/R_{\text{standard}}) - 1] \times 1,000$ ($R = {}^{13}\text{C}/{}^{12}\text{C}$ or D/H) and are reported relative to internationally recognized standards Vienna Pee Dee Belemnite (VPDB) (${}^{13}\text{C}/{}^{12}\text{C}$) and Vienna Standard Mean Ocean Water (VSMOW) (D/H) as established by the International Atomic Energy Agency in Vienna, Austria (36)].

Inverse Modeling. We optimized monthly emission rates by seven processes and by geographic region for wetlands and biomass burning resulting in ten source categories [wetlands (90°S–0, 0–30°N, and 30°N–90°N), biomass burning (separated according to C3/C4 vegetation distribution), gas and oil, coal, livestock, waste, and rice agriculture] using a fixed-lag Kalman smoother method (37, 38). The independence of source categories was evaluated through source covariance; results of this analysis indicate that correlations were weak for all paired sources ($|r| < 0.15$), implying that inversion sources are largely independent. We calculated response functions for the inversion using the chemical-transport model GEOS-Chem run at a horizontal resolution of $4^\circ \times 5^\circ$. The base inversion included sinks due to reaction with OH, soil uptake, and stratospheric loss. Spatially gridded monthly varying prior emissions fields were constructed from a number of sources (SI Appendix, section S.3.1) (8, 39, 40). We calculated monthly mean CH_4 mixing ratios (1984–2009) from the NOAA Earth System Laboratory's GLOBALVIEW-CH4 data product by sampling cubic spline fits to the weekly records (221 locations and 24 ship sites) at daily frequency (19). ${}^{13}\text{CH}_4$ was

introduced to the model as an independent tracer with source signatures drawn from previous work (SI Appendix, Table S1). To our air archive $\delta^{13}\text{C}$ measurements we added 13 stations from Institute of Arctic and Alpine Research (INSTAAR) and extended back five stations (South Pole; Tutuila, American Samoa; Mauna Loa, HI; Cape Grim, Tasmania; Point Barrow, AK) to 1988 using Quay et al. (16). Additional $\delta^{13}\text{C}$ measurements by Quay et al. (16) at Cheeka Peak, WA, and Baring Head, New Zealand, and by Tyler et al. (17) at Niwot Ridge, CO, and Montaña de Oro, CA, were also used (for a full list of $\delta^{13}\text{C}$ observations, see SI Appendix, Table S3). To test the sensitivity of the retrieved source strengths and trends to the inversion setup we performed 53 inversions under different inversion scenarios (SI Appendix, section S.6). A full description of the inversion setup and sensitivity tests is available in the SI Appendix.

ACKNOWLEDGMENTS. We thank Paul Quay, Stanley Tyler, NOAA-ESRL GLOBALVIEW- CH_4 , and INSTAAR for their published CH_4 concentration and isotopic datasets (1984–2010) and for isotopic calibration standards. We thank Mariela Brooks and Katie Brennan for laboratory measurements, Erica Hanson for preliminary modeling, and the constructive comments of anonymous reviewers. This work was supported by the US National Science Foundation (Atmospheric and Geospace Sciences Grant 0952307) and the Miller Foundation and MJ Murdock Charitable Trust (Grant 2012183) for computing infrastructure.

- Hartmann DL, et al. (2013) Observations: Atmosphere and surface. *Climate Change 2013: The Physical Science Basis. Contribution of Working Group I to the Fifth Assessment Report of the Intergovernmental Panel on Climate Change*, eds Stocker TF, et al. (IPCC, Cambridge, UK).
- Myhre G, et al. (2013) Anthropogenic and natural radiative forcing. *Climate Change 2013: The Physical Science Basis. Contribution of Working Group I to the Fifth Assessment Report of the Intergovernmental Panel on Climate Change*, eds Stocker TF, et al. (IPCC, Cambridge, UK).
- Kirschke S, et al. (2013) Three decades of global methane sources and sinks. *Nat Geosci* 6(10):813–823.
- Dlugokencky EJ, et al. (2003) Atmospheric methane levels off: Temporary pause or new steady-state? *Geophys Res Lett* 30(19): 10.1029/2003GL018126.
- Khalil MAK, Butenhoff CL, Rasmussen RA (2007) Atmospheric methane: Trends and cycles of sources and sinks. *Environ Sci Technol* 41(7):2131–2137.
- Aydin M, et al. (2011) Recent decreases in fossil-fuel emissions of ethane and methane derived from firm air. *Nature* 476(7359):198–201.
- Simpson IJ, et al. (2012) Long-term decline of global atmospheric ethane concentrations and implications for methane. *Nature* 488(7412):490–494.
- EDGAR (2011) *Emission Database for Global Atmospheric Research (EDGAR) (version 4.2)* (European Commission Joint Research Centre/Netherlands Environmental Assessment Agency). Available at edgar.jrc.ec.europa.eu. Accessed August 29, 2016.
- Kai FM, Tyler SC, Randerson JT, Blake DR (2011) Reduced methane growth rate explained by decreased Northern Hemisphere microbial sources. *Nature* 476(7359):194–197.
- Kai FM, Tyler SC, Randerson JT (2010) Modeling methane emissions from rice agriculture in China during 1961–2007. *J Integr Environ Sci* 7:49–60.
- Khalil MAK, Shearer MJ (2006) Decreasing emissions of methane from rice agriculture. *Int Congr Ser* 1293:33–41.
- Levin I, et al. (2012) No inter-hemispheric $\delta^{13}\text{CH}_4$ trend observed. *Nature* 486(7404):E3–E4, discussion E4.
- Schaefer H, et al. (2016) A 21st-century shift from fossil-fuel to biogenic methane emissions indicated by ${}^{13}\text{CH}_4$. *Science* 352(6281):80–84.
- Francey RJ, et al. (1999) A history of $\delta^{13}\text{C}$ in atmospheric CH_4 from the Cape Grim air archive and Antarctic firm air. *J Geophys Res* 104(D19):23631–23643.
- Monteil G, et al. (2011) Interpreting methane variations in the past two decades using measurements of CH_4 mixing ratio and isotopic composition. *Atmos Chem Phys* 11(17):9141–9153.
- Quay P, et al. (1999) The isotopic composition of atmospheric methane. *Global Biogeochem Cycles* 13(2):445–461.
- Tyler SC, Rice AL, Ajie HO (2007) Stable isotope ratios in atmospheric CH_4 : Implications for seasonal sources and sinks. *J Geophys Res* 112(D03303): 10.1029/2006JD007231.
- Bey I, et al. (2001) Global modeling of tropospheric chemistry with assimilated meteorology: Model description and evaluation. *J Geophys Res* 106(D19):23073–23095.
- GLOBALVIEW-CH4 (2009) *GLOBALVIEW-CH4: Cooperative Atmospheric Data Integration Project - Methane* (NOAA ESRL, Boulder, CO).
- White JWC, Vaughn BH, Michel SE (2015) *Stable Isotopic Composition of Atmospheric Methane (${}^{13}\text{C}$) from the NOAA ESRL Carbon Cycle Cooperative Global Air Sampling Network, 1998–2014*. (University of Colorado, Institute of Arctic and Alpine Research [INSTAAR], Boulder, CO).
- Dlugokencky EJ, Nisbet EG, Fischer H, Lowry D (2011) Global atmospheric methane: Budget, changes and dangers. *Phil Trans R Soc A* (369):2058–2072.
- Bousquet P, et al. (2006) Contribution of anthropogenic and natural sources to atmospheric methane variability. *Nature* 443(7110):439–443.
- Granié C, et al. (2011) Evolution of anthropogenic and biomass burning emissions of air pollutants at global and regional scales during the 1980–2010 period. *Clim Change* 109(1–2):163–190.
- Giglio L, Randerson JT, van der Werf GR (2013) Analysis of daily, monthly, and annual burned area using the fourth-generation global fire emissions database (GFED4). *J Geophys Res* 118(1):317–328.
- Yang J, et al. (2014) Spatial and temporal patterns of global burned area in response to anthropogenic and environmental factors: Reconstructing global fire history for the 20th and early 21st centuries. *J Geophys Res* 119(3):249–263.
- Howarth R, Santoro R, Ingraffea A (2011) Methane and the greenhouse-gas footprint of natural gas from shale formations. *Clim Change* 106:679–690.
- Stern DI, Kaufmann RK (1996) Estimates of global anthropogenic methane emissions 1860–1993. *Chemosphere* 33(1):159–176.
- Mieville A, et al. (2010) Emissions of gases and particles from biomass burning during the 20th century using satellite data and an historical reconstruction. *Atmos Environ* 44(11):1469–1477.
- Spahni R, et al. (2011) Constraining global methane emissions and uptake by ecosystems. *Biogeosciences* 8(6):1643–1665.
- Bogner J, Matthews E (2003) Global methane emissions from landfills: New methodology and annual estimates 1980–1996. *Global Biogeochem Cycles* 17(2):1065–1069.
- FAOSTAT (2016) *Food and Agriculture Organization of the United Nations Statistics Division* (United Nations, Rome). Available at faostat.fao.org. Accessed August 29, 2016.
- Akagi SK, et al. (2011) Emission factors for open and domestic biomass burning for use in atmospheric models. *Atmos Chem Phys* 11(9):4039–4072.
- Dlugokencky EJ, et al. (2005) Conversion of NOAA atmospheric dry air methane mole fractions to a gravimetrically-prepared standard scale. *J Geophys Res* 110(D18306): 10.1029/2005JD006035.
- Rice AL, Gotthard AA, Ajie HO, Tyler SC (2001) High-precision continuous-flow measurement of $\delta^{13}\text{C}$ and δD of atmospheric CH_4 . *Anal Chem* 73(17):4104–4110.
- Teama DG (2013) A 30-year record of the isotopic composition of atmospheric methane. Ph.D. Dissertation (Portland State University, Portland, Oregon).
- Coplen TB (1995) Reporting of stable carbon, hydrogen, and oxygen isotopic abundances. *Reference and Inter-Comparison Materials for Light Elements* (IAEA, Vienna, Austria), pp 31–34.
- Bruhwiller LMP, Michalak AM, Peters W, Baker DF, Tans P (2005) An improved Kalman smoother for atmospheric inversions. *Atmos Chem Phys* 5(10):2691–2702.
- Chen YH, Prinn RG (2006) Estimation of atmospheric methane emissions between 1996 and 2001 using a three-dimensional global chemical transport model. *J Geophys Res* 111:D10307.
- Giglio L, et al. (2010) Assessing variability and long-term trends in burned area by merging multiple satellite fire products. *Biogeosciences* 7:1171–1186.
- Pickett-Heaps CA, et al. (2011) Magnitude and seasonality of wetland methane emissions from the Hudson Bay Lowlands (Canada). *Atmos Chem Phys* 11(8): 3773–3779.